JOURNAL OF MATERIALS SCIENCE 18 (1983) 2777–2784

A study of the electrical characteristics, before electroforming, of thin SiO_x films with laterally-spaced electrodes

S. A. Y. AL-ISMAIL, C. A. HOGARTH
Department of Physics, Brunel University, Uxbridge, Middlesex, UK

The sample structure comprises two laterally-spaced electrodes joined by a thin dielectric film. The electrodes make a blocking contact to the dielectric with a barrier height ~ 0.75 eV. The voltage–current characteristic is studied between 213 to 413 K. Below room temperature the effect of hopping conduction on such contacts is explained. At room temperature and at high fields where hopping conduction is expected to be less effective, the conduction is controlled by the contact. Above room temperature and at low fields localized state conduction (hopping) becomes effective again with activation energy ~ 0.07 eV and an estimated charge carrier mobility of $1.3 \times 10^{-2}\,cm^2\,V^{-1}\,sec^{-1}$. The density of ionizable impurities is estimated to be in the range 1 to $6 \times 10^{18}\,cm^{-3}$ and the density of surface states is of the order of $1 \times 10^{13}\,cm^{-2}$.

1. Introduction

Silicon monoxide has been used widely in technology as a dielectric in thin film capacitors and as a passivating layer. As an active material it has been used in thin film M–SiO_x–M structures (M = metal), and after electroforming it shows voltage-controlled negative resistance (VCNR), electron emission and memory effects [1–4]. Before forming, samples subjected to high electric fields usually show a log $I_c \propto V_b^{1/2}$ dependence [1], where I_c is the circulating current through the device and V_b is the applied voltage. Such behaviour is normally indicative of Schottky or Poole–Frenkel effects. In the conventional SiO_x sandwich structures the conduction is believed to be controlled by the bulk material and to conform with the equations describing the Poole–Frenkel effect, while Schottky emission, i.e. the dependence of the V_b–I_c characteristic at high fields primarily on the electrode material, has been discounted in SiO_x films [5–8]. However, in the interpretation of the results to be described in this paper, the equations for the Poole–Frenkel effect or even their modified versions give inconsistent parameters, and it is suggested some other barrier lowering mechanism at impurity sites may be involved [9, 10].

It has been reported [11] that discontinuous gold films on an insulating substrate in a planar arrangement showed a non-ohmic V_b–I_c characteristic, before electroforming, and this was attributed to Schottky emission as the main high-field transport mechanism with space-charge effects and tunnelling from island to island taking place.

In this work the samples are SiO_x films between metal electrodes, laterally spaced, in a planar arrangement. The voltage–current characteristic before electroforming is studied in the temperature range 213–413 K. Nonlinear V_b–I_c behaviour is noticed and explained in terms of Schottky emission due to a blocking contact as the dominant process, with hopping conduction also taking place particularly at low temperatures. At higher temperatures and at the lower fields the contribution from hopping conduction becomes more important.

2. Experimental technique

2.1. Preparation of samples

Cu–SiO_x–Cu thin film structures were deposited on Corning 7059 glass substrates held at a temperature of ~ 150° C in a vacuum of 1 to 5×10^{-6} torr using a Balzers BA 510 coating unit. Molybdenum or tantalum boats were used for evaporating

0022–2461/83 $03.00 + .12

the materials. Evaporation rates were monitored by an Edwards quartz crystal monitor device and these were generally 0.8 to 1.0 nm sec^{-1} (Copper) and 0.6 to 0.7 nm sec^{-1} (SiO_x). Up to ten samples were fabricated on each substrate. Configurations different from the conventional MIM sandwich, were employed in our study and are shown in Fig. 1 where the electrodes are laterally spaced. This configuration is created by the simple technique of fixing a wire in the path of the evaporating metal atoms which leaves a central region literally clear of deposited metal but which also gives rise to two penumbral regions. Initially a thin dielectric layer (10 to 12 nm) was evaporated onto the substrate before evaporating the electrodes, thereby reducing any substrate effect on the effective area and then on the top of the electrode edges a thick layer of dielectric was evaporated to fill the gap between the electrodes and to cover the edges of the effective area.

The layer thicknesses were measured using a M 100 Ångstrømeter multibeam interferometer. The geometrical separation between the electrodes was measured using a Reichert–Jung Microstar 110 optical microscope.

2.2. Electrical measurements

Electrical measurements were performed in a vacuum system maintained at a pressure of 10^{-6} to 10^{-5} torr. The d.c. bias voltage was provided by a Coutant LB 500.2 power supply and the current was recorded by an electronic Avometer EA 113. The voltage across the sample was monitored by a digital voltmeter. The temperature was lowered by firmly attaching the substrate to a brass enclosure containing liquid nitrogen. Intermediate temperatures between -60 and 130° C could be obtained by using this in conjunction with a small resistive heater. Sample temperatures were monitored with a small chromel–alumel thermocouple attached to the substrate. The dielectric constant could be calculated after measuring the capacitance, using a Wayne Kerr Autobalance Universal Bridge B641.

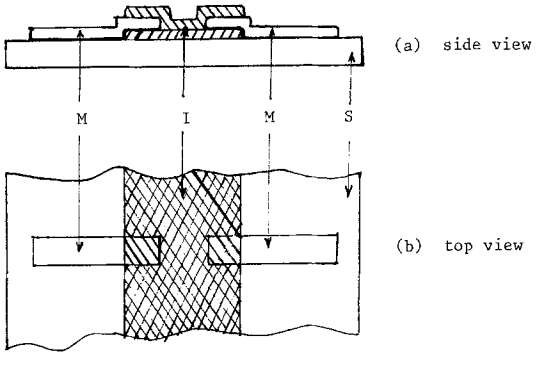

Figure 1 Device structure: M–metal electrode, I–insulator, S–substrate.

3. Results and discussion

In these samples reasonable and consistent values of parameters were obtained if we use as parameter an effective electrode separation d_{eff} and effective area A_{eff} in the calculations instead of the geometrically calculated values d_{geom} and A_{geom}, where $d_{eff} < d_{geom}$ and $A_{eff} > A_{geom}$. Considering the dimensions of the boat and the mask and their distance from the substrate where a penumbra is expected, it is found that

$$d_{eff} = \left(\frac{h_1}{h_2} - 1\right)\beta - \frac{h_1}{h_2}\alpha \qquad (1)$$

where h_1 and h_2 are the heights of the substrates and of the mask from the boat, respectively, β is the boat width and α is the width of the wire (obstacle).

3.1. Voltage–current dependence at low temperature

A point of interest is the nonlinear dependence of current on voltage as shown in Fig. 2. The interpretation of these curves based on the assumption of a simple Poole–Frenkel or Schottky effect (i.e. by plotting log I_c against $V_b^{1/2}$) leads to values of parameters incompatible with the theory and to unreasonably low values of dielectric constant. Good theoretical agreement with the results is obtained on the assumption that a blocking contact exists, leading to a modified form of Schottky emission. At such contacts a space charge will be created in a depletion region due to the difference in the work functions of the metal and of the insulator and if there is an adequate density of donors N_d (positive when empty) in the insulator, then electrons will be emitted from these states into the metal until thermochemical equilibrium is achieved. This depletion region will extend to a distance λ and will give rise to an electric field in the region much higher than in the bulk. The depletion region is more resistive than the rest of the bulk due to the absence of mobile carriers and the applied potential difference will almost entirely drop across this region. The electric field E and subsequently the field-lowering contact barrier $\Delta\phi$ are determined by the depletion width

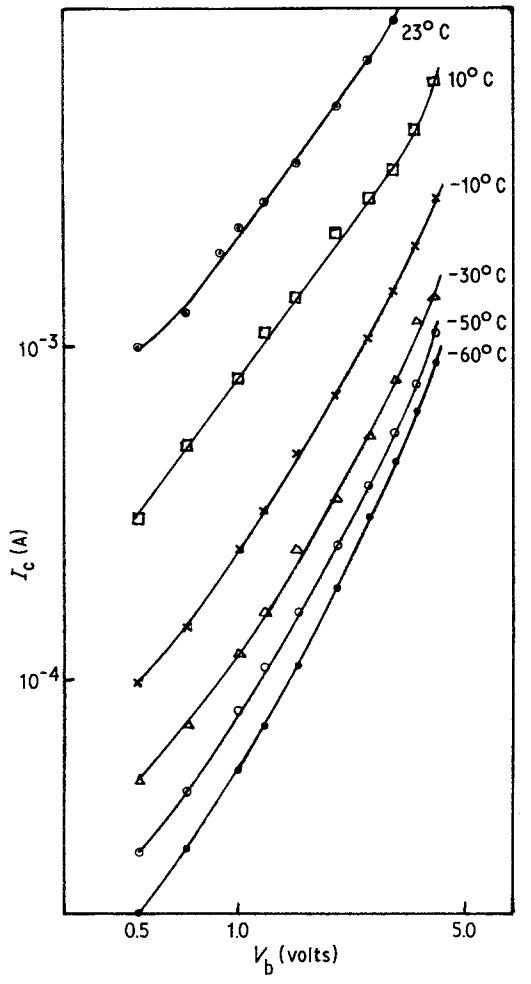

Figure 2 Voltage–current characteristics for a planar sample at several temperatures showing the absence of ohmic conduction.

λ, which in turn is determined by the density N_d of ionizable impurities according to the relation [12-15]

$$\lambda = \left(\frac{2\epsilon_0 \epsilon_r V_c}{qN_d}\right)^{1/2} \simeq 1052 \left(\frac{\epsilon_r V_c}{N_d}\right)^{1/2} \quad (2)$$

where V_c is the effective potential across the contact, $q = 1.6 \times 10^{-19}$ C, $\epsilon_0 = 8.854 \times 10^{-14}$ F cm^{-1} and ϵ_r is the relative dielectric constant. The dielectric field at this contact is given by

$$E_c = \left(\frac{2qN_d V_c}{\epsilon_0 \epsilon_r}\right)^{1/2} \simeq 1.9 \times 10^{-3} \left(\frac{V_c N_d}{\epsilon_r}\right)^{1/2} \quad (3)$$

The interaction of this field with the image force lowers the contact barrier by an amount $\Delta\phi$ given by

$$\Delta\phi = q\left(\frac{q^3 N_d V_c}{2(8\pi)^2 \epsilon_0^3 \epsilon_r^3}\right)^{1/4} \simeq 8.26 \times 10^{-6} q \left(\frac{N_d V_c}{\epsilon^3}\right)^{1/4} \quad (4)$$

Since the potential drop across λ is V_c then the relation governing the emission current, which is independent of the insulator thickness, is of the form [12]

$$I_c = AA^*T^2 \times \exp\left[-\frac{\phi - 8.26 \times 10^{-6} q(N_d V_b/\epsilon_r^3)^{1/4}}{kT}\right] \quad (5)$$

where A is the effective area, A^* is the effective Richardson–Dushman constant, T is the absolute temperature, k is the Boltzmann constant (8.62×10^{-5} eV K^{-1}) and ϕ is the contact-barrier height. V_b is the applied voltage (assumed, approximately, equal to V_c).

The surface density of charge N_s per unit area, which is required to screen the internal field E_c is given by [15]

$$N_s = \lambda N_d \quad (6)$$

Using Equation 5, a plot of $\log I_c$ against $V_b^{1/4}$ would give the value of N_d. This plot is shown in Fig. 3. Using Equations 2 to 6, the average values of the parameters are $N_d \simeq 6 \times 10^{18}$ cm^{-3}, $\lambda \simeq 2 \times 10^{-6}$ cm, $E_c \simeq 4 \times 10^6$ V cm^{-1} and $N_s \simeq 1.1 \times 10^{13}$ cm^{-2}. The contact-barrier height is found to be 0.55 eV as shown in Fig. 4.

3.2. Temperature dependence of current through the blocking contact

The effects of temperature on such a contact are studied over the same range of voltages. According to Equation 5, a plot of $\log(I_c/T^2)$ against $1/T$ is shown in Fig. 5. If the transfer of electrons is only through such a contact then a straight line would be expected to satisfy the equation, but in Fig. 5 a transition from a straight line with low gradient to one with a higher gradient, as the temperature is increased from 213 to 296 K, is seen. The transition is gradual and takes place within the temperature range -8 to $-13°$ C. This suggests that more than one conduction mechanism is involved. The curves in Fig. 5 produced parameters whose values were consistent with results from the previous section, i.e. $\phi_0 \simeq 0.55$ eV and $N_d \simeq 6 \times 10^{18}$ cm^{-3}.

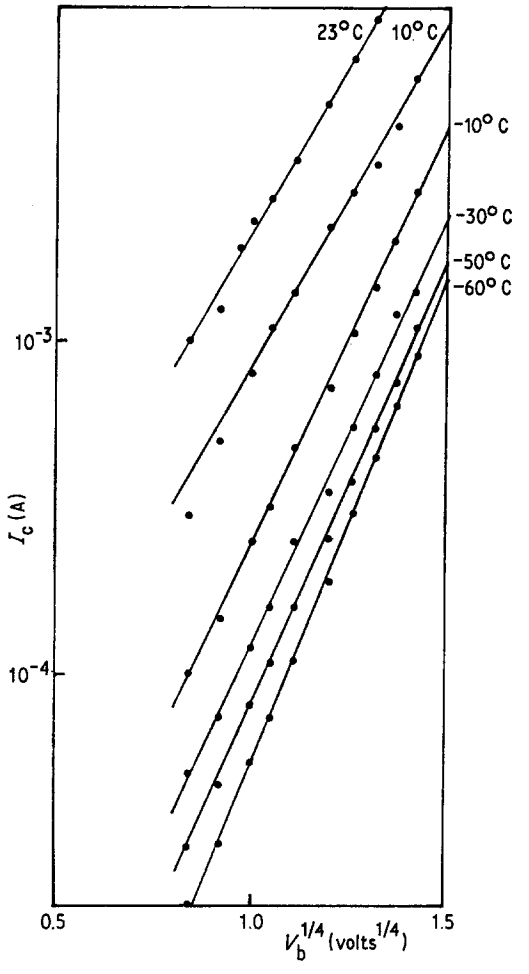

Figure 3 Data from Fig. 2 analysed on the assumption of the existence of a blocking contact.

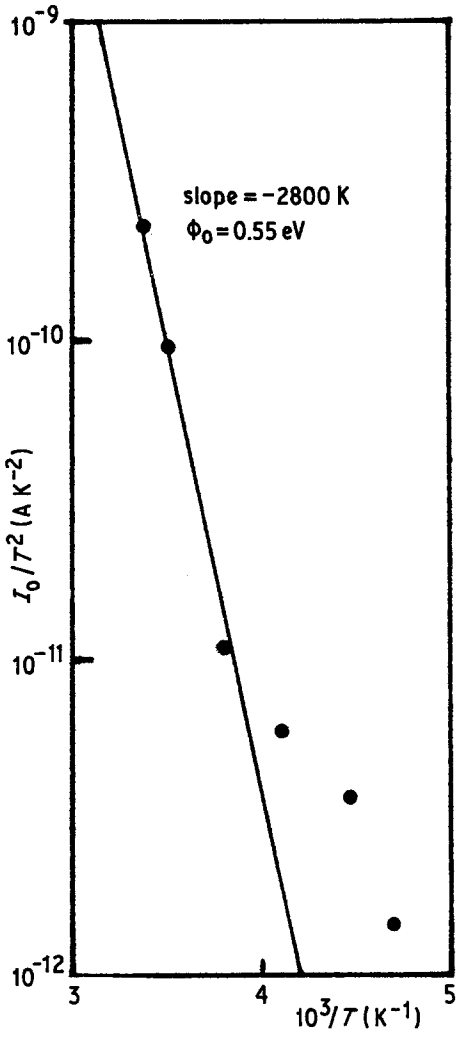

Figure 4 The intercept of I_c at $V_b = 0$ in Fig. 3 plotted against $1/T$. Intercept of I_0/T^2 at $1/T = 0$ is 0.46 A K^{-2}.

The high density of donor centres which exists in the bulk of the SiO_x may affect the conduction in certain temperature ranges.

Fig. 6 shows a plot of $\log I_c$ against $1/T$ which has no significant influence on the gradients compared to Fig. 5, but the lower part is more pronounced and gave activation energy values in the range 0.07 to 0.14 eV. These low activation energies may be attributed to hopping conduction, which is expected at such low temperatures.

If the contribution of hopping current is subtracted from the total current, then the remaining component of current should be due to the contact-barrier lowering. This plot is shown in Fig. 7 where the gradients of the straight lines yield activation energies between 0.54 and 0.68 eV according to the bias voltage. Fig. 8 shows the plot of the activation energies against $V_b^{1/4}$; the slope yields $N_d \simeq 6.56 \times 10^{18}\,cm^{-3}$ and $\epsilon_r \simeq 4.85$, values which are consistent with the previous results, within the accuracy of the measurements. The intercept at $V_b = 0$ gives a contact-barrier height of 0.75 eV, which is higher than the previous result (0.55 eV). We can see that the bulk conduction (hopping) can affect the calculation of the height of the barrier at the contact by at least 0.2 eV. Moreover, considering the effect of surface states the actual contact-barrier height is expected to be fractionally higher.

At room temperature and higher fields where the hopping conduction is expected to be reduced, the barrier height was calculated to be equal to 0.7 eV and the characteristic is shown in Fig. 9. The density of donors is $\sim 1.34 \times 10^{18}\,cm^{-3}$ and the depletion region thickness is $\sim 7.2 \times 10^{-6}$ cm. We notice that there is a gradual decrease in the

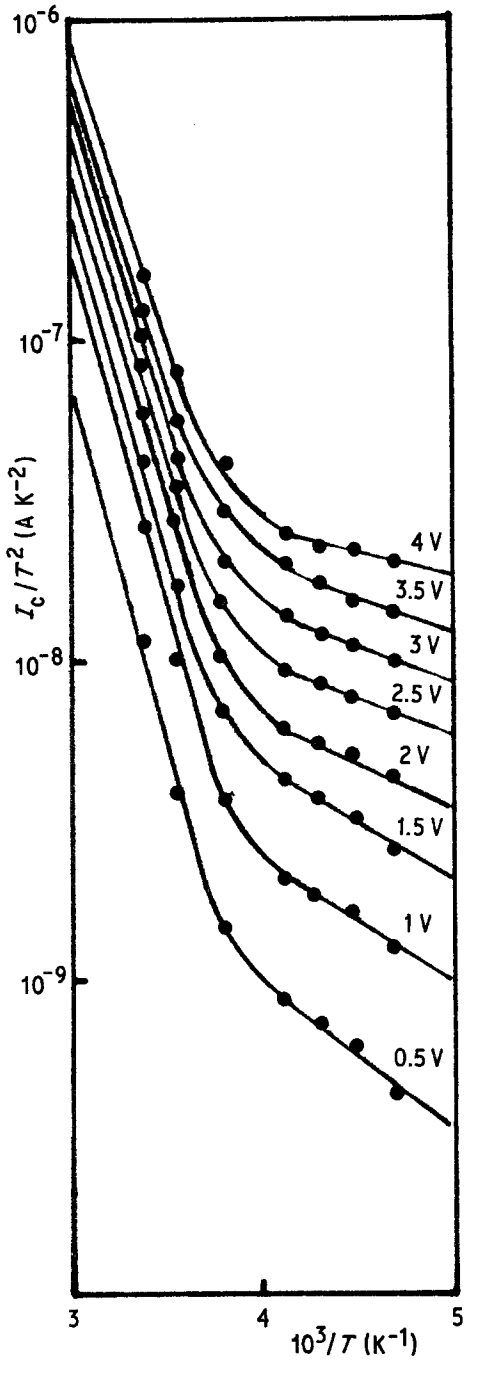

Figure 5 Temperature dependence of a blocking current at different voltages.

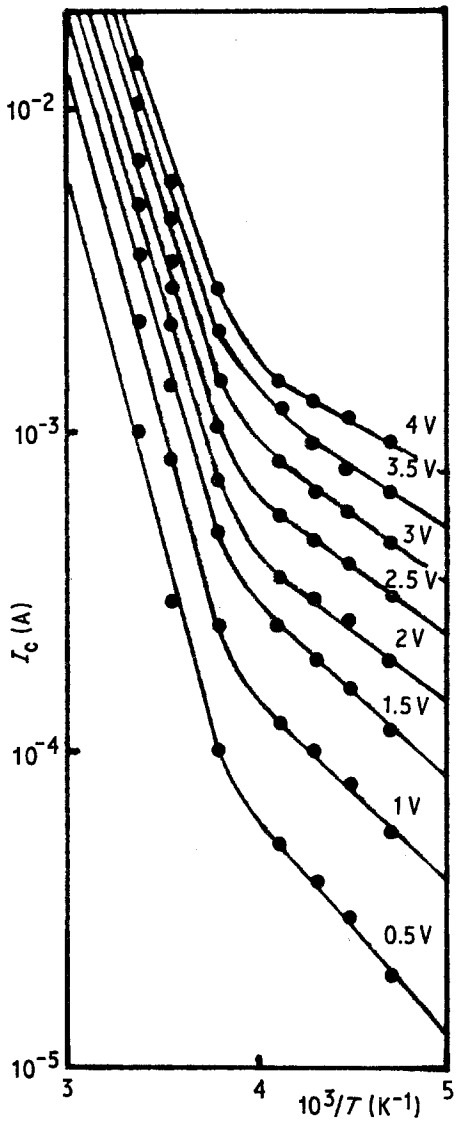

Figure 6 Current as a function of inverse temperature showing a transition from hopping to contact-controlled conduction.

slope at about 12.5 V accompanied by a decrease of the barrier height to 0.62 eV and the depletion region was then estimated as somewhat wider (13.2×10^{-6} cm). The surface state density at lower voltages is $\sim 9.7 \times 10^{12}$ cm^{-2}, while at higher voltages this quantity takes on a higher value of approximately 1.8×10^{13} cm^{-2}. This decrease in the slope may involve yet another mechanism at higher fields.

A comparison between the two sets of samples E7S10 and E7S11 is shown in Fig. 10, which displays the $I_c - V_b$ characteristics at low voltages and at room temperature. The higher the current level the higher is the donor density and density of states, and the narrower the depletion region.

If we assume that the depletion regions penetrate to a distance $\lambda \simeq d/2$, then, according to our results, the necessary pinch-off voltage would be around 1 MV for devices No. E7S10 and as high as 5 MV for devices No. E7S11 depending on N_d.

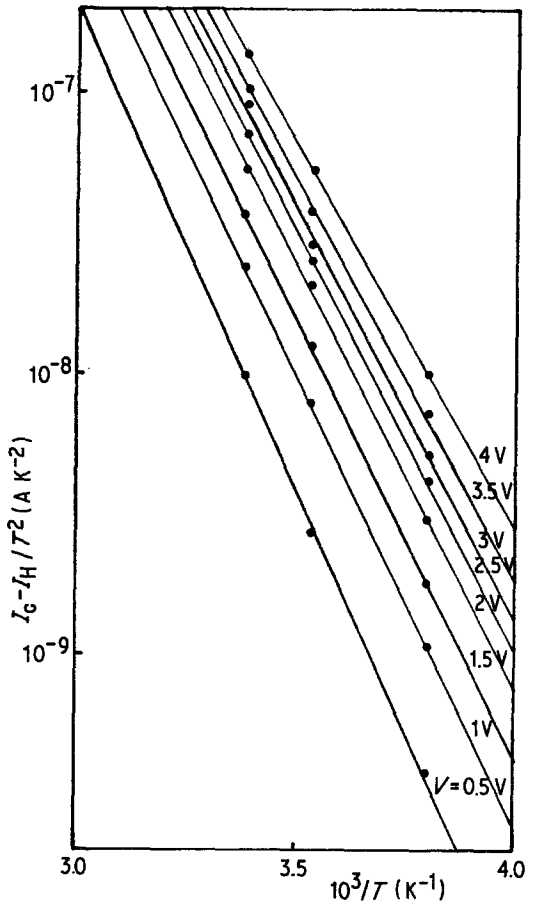

Figure 7 The difference between total current and hopping current as a function of inverse temperature at various applied voltages.

3.3. High-temperature and low-field characteristics

A typical $I_c - V_b$ characteristic is shown in Fig. 11 and is ohmic up to ~ 3 V. The current at low field

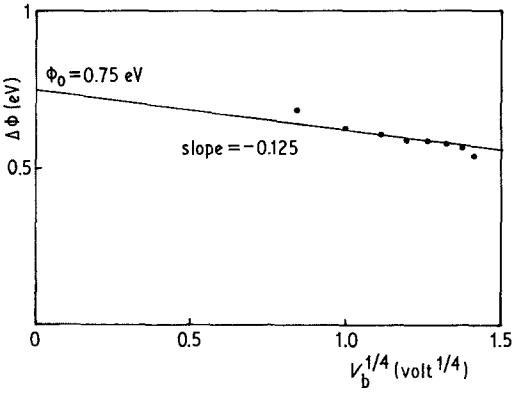

Figure 8 The activation energy, calculated from Fig. 7 as a function of $V_b^{1/4}$. The barrier height at $V_b = 0$ is $\phi_c = 0.75$ eV.

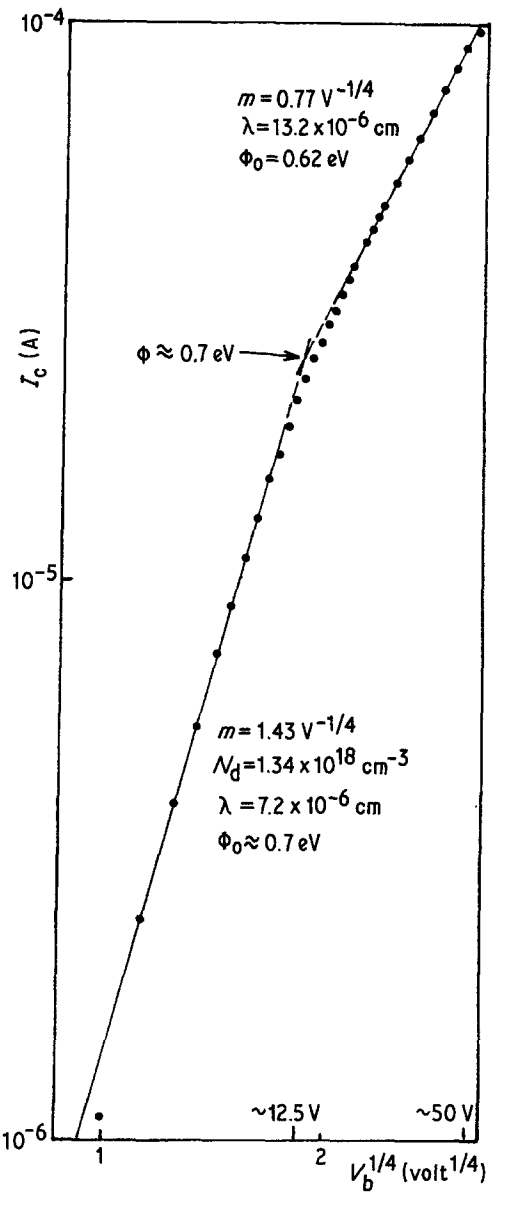

Figure 9 Current as a function of $V_b^{1/4}$ at room temperature for a planar sample.

varies with temperature in accordance with the equation

$$I_c = I_0 \exp(-\Delta E/kT) \tag{7}$$

where ΔE is the activation energy for donors or traps, and

$$I_0 = q\mu N_d \frac{V_b}{d} A \tag{8}$$

where q is the electronic charge, μ is the mobility, N_d is the impurity density, V_b is the bias voltage, d is the effective electrode separation and A is the effective area.

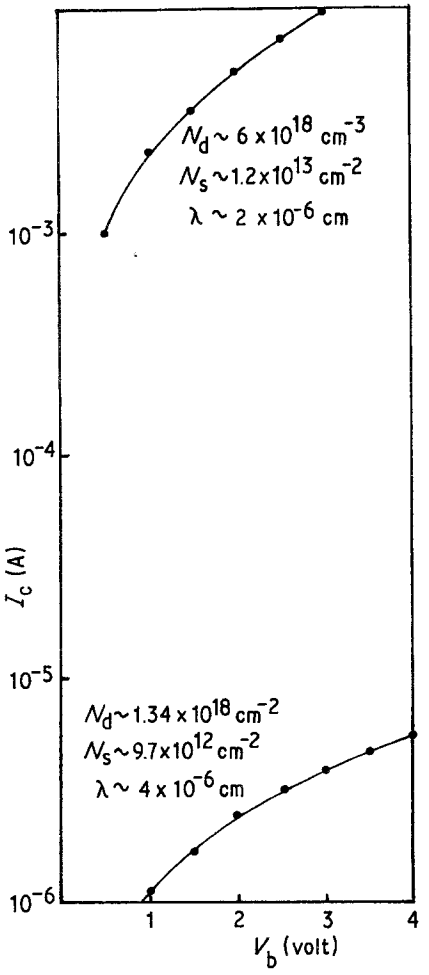

Figure 10 Comparison between two sets of devices, showing the parameters which affect the current level at room temperature.

A plot of $\log I_c$ against $1/T$ is shown in Fig. 12. According to Equation 7 the gradients for these slopes yield a consistent value of activiation energy, $\Delta E \simeq 0.07$ eV, at different voltages. Using $N_d \simeq 6 \times 10^{18}$ cm^{-3} the mobility was estimated to be 1.3×10^{-2} cm^2 V^{-1} sec^{-1}. This low value of mobility and activation energy with an ohmic I_c–V_b characteristic is an indication of a localized state conduction (hopping) at low fields and high temperature.

4. Conclusions

A blocking contact occurs in our planar geometry samples due to a high density of ionizable impurities $\sim 6 \times 10^{18}$ cm^{-3}. As a result a positive space-charge layer forms at the electrodes with a density high enough to terminate most lines of force from the electrodes and thereby absorb most of the applied

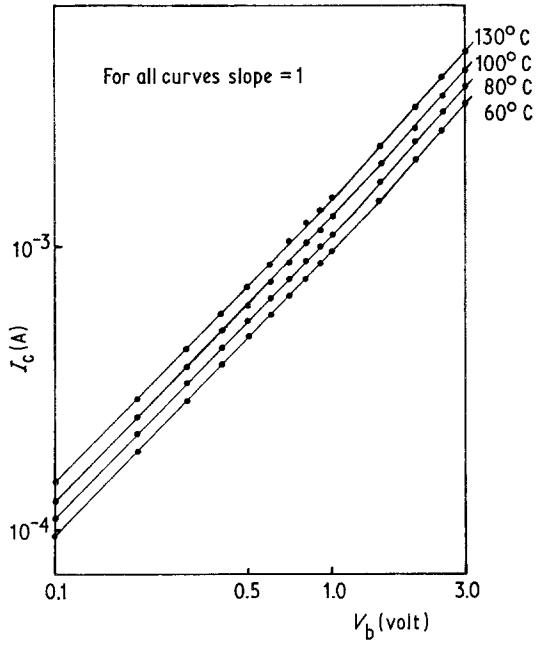

Figure 11 Voltage–current characteristics of sample E7S11D4 above room temperature.

voltage. The electric field at the contact becomes thickness independent and will be determined by the impurity or donor density. The depletion layer thickness of $\sim 2 \times 10^{-6}$ cm is established with a barrier height of 0.7 to 0.75 eV at the contact. This barrier will be affected by hopping conduction at lower temperatures by 0.2 eV. The estimated hopping mobility of 1.3×10^{-2} cm^2 V^{-1} sec^{-1} is associated with a 0.07 eV activation energy at higher temperatures. The breakthrough voltage is inversely proportional to the donor density and density of surface states, and this feature is

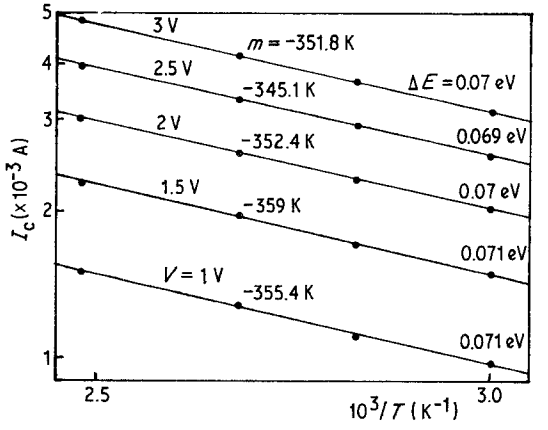

Figure 12 I_c as a function of inverse temperature for various applied voltages for the sample described in Fig. 11.

important in the fabrication of microelectronic circuits.

In further publications we shall show that such devices may be electroformed and display VCNR analogous to the normal MIM sandwich structures.

A major advantage of the planar structure is that direct electron microscope observation is possible.

References

1. J. G. SIMMONS and R. R. VERDERBER, *Proc. Roy Soc.* **A301** (1967) 77.
2. R. R. VERDERBER, J. G. SIMMONS and B. EALES, *Phil. Mag.* **16** (1967) 1049.
3. R. A. COLLINS and R. D. GOULD, *Solid State Elect.* **14** (1971) 805.
4. R. D. GOULD and C. A. HOGARTH, *Int. J. Elect.* **37** (1974) 157.
5. A. K. JONSCHER and A. A. ANSARI, *Phil. Mag.* **23** (1971) 205.
6. H. HIROSE and Y. WADA, *Jpn. J. Appl. Phys.* **3** (1964) 179.
7. T. E. HARTMAN, J. G. BLAIR and R. BAUER, *J. Appl. Phys.* **37** (1966) 2468.
8. M. STUART, *Brit. J. Appl. Phys.* **18** (1967) 1637.
9. P. A. TIMSON and C. A. HOGARTH, *Thin Solid Films* **5** (1971) R33.
10. R. D. GOULD and C. A. HOGARTH, *Int. J. Elect.* **38** (1975) 577.
11. R. BLESSING and H. PAGNIA, *Thin Solid Films* **52** (1978) 333.
12. J. G. SIMMONS, *J. Phys. D. Appl. Phys.* **4** (1971) 613.
13. *Idem, Phys. Rev.* **166** (1968) 912.
14. *Idem,* "Handbook of Thin Film Technology", edited by L. I. Maissel and R. Glang (McGraw-Hill, New York, 1970) Chap. 14.
15. A. K. JONSCHER and R. M. HILL, "Physics of Thin Films" Vol. 8, edited by G. Hass, M. H. Francombe and R. W. Hoggman (Academic Press, London, New York 1975) p. 169.

Received 25 January
and accepted 15 February 1983